Drainage basin responses to climate change

Gregory E. Tucker

Ralph M. Parsons Laboratory, Massachusetts Institute of Technology, Cambridge

Rudy Slingerland

Department of Geosciences and Earth System Science Center, Pennsylvania State University, University Park

Abstract.   Recent investigations have shown that the extent of the channel network in some drainage basins is controlled by a threshold for overland flow erosion. The sensitivity of such basins to climate change is analyzed using a physically based model of drainage basin evolution. The GOLEM model simulates basin evolution under the action of weathering processes, hillslope transport, and fluvial bedrock erosion and sediment transport. Results from perturbation analyses reveal that the nature and timescale of basin response depends on the direction of change. An increase in runoff intensity (or a decrease in vegetation cover) will lead to a rapid expansion of the channel network, with the resulting increase in sediment supply initially generating aggradation along the main network, followed by downcutting as the sediment supply tapers off. By contrast, a decrease in runoff intensity (or an increase in the erosion threshold) will lead to a retraction of the active channel network and a much more gradual geomorphic response. Cyclic changes in runoff intensity are shown to produce aggradational-degradational cycles that resemble those observed in the field. Cyclic variations in runoff also lead to highly punctuated denudation rates, with denudation concentrated during periods of increasing runoff intensity and/or decreasing vegetation cover. The sediment yield from threshold-dominated basins may therefore exhibit significant variability in response to relatively subtle environmental changes, a finding which underscores the need for caution in interpreting modern sediment-yield data.

Introduction

Understanding how climate change impacts the fluvial landscape is essential for predicting the impact of future changes in climate and land use as well as for deciphering the geomorphic and stratigraphic record of climate change. Traditionally, efforts to understand the connection between climate change and drainage basin response have been historical in nature, focusing on the Quaternary record of landscape change [e.g., *Vita-Finzi*, 1969; *Knox*, 1972, 1983, 1984; *Brakenridge*, 1980; *Smith*, 1982; *Dorn et al.*, 1987; *Dohrenwend*, 1987; *Blum and Valastro*, 1989; *Hall*, 1990; *Bull*, 1991; *Meyer et al.*, 1992; *Sugai*, 1993; *Arbogast and Johnson*, 1994]. Studies such as these have provided a wealth of empirical, albeit sometimes contradictory, information about the net geomorphic (and especially fluvial) response to changes in mean climate conditions in different regions. Because of the complex and coupled nature of the geomorphic system, however, such studies shed relatively little light on the physical mechanisms and feedbacks that lead to any given observed geomorphic patterns. Only recently have these issues begun to be addressed in a quantitative framework [e.g., *Freeze*, 1987; *Slingerland and Snow*, 1988; *Montgomery and Dietrich*, 1989, 1992, 1994; *Willgoose et al.*, 1991; *Dietrich et al.*, 1992, 1993; *Kirkby*, 1994; *Willgoose*, 1994; *Rinaldo et al.*, 1995; *Howard*, 1996], and a number of important questions remain: What factors determine whether a valley network will undergo erosion or aggradation in response to a given climate

or land-use change? What is the role of interactions between channel and hillslope processes? How might geomorphic responses vary in different parts of a drainage basin and through time? And how might responses vary as a function of the timescale of change? The answers to these questions are important both for proper interpretation of the geomorphic record of climate change and for predicting the impact of future changes.

The goal of this study is to model the response of a "typical" midlatitude watershed to changes in runoff and in surface resistance to erosion by running water. We do not consider the full range of drainage basin types, with varying relief, processes, and other factors, but instead restrict the analysis to the case of moderate-relief, threshold-dominated basins. "Moderate relief" implies a basin in which mass movement is not a significant process, while "threshold-dominated" refers to basins in which channels form only where overland flow generates sufficient shear stress to initiate erosion [*Horton*, 1945; *Montgomery and Dietrich*, 1989]. The issue of channel initiation is a central one in the context of climate change. The extent of an active channel network, which influences the degree of landscape dissection, may be especially sensitive to climate change [*Montgomery and Dietrich*, 1992]. Depending on the setting, channel network extent may be controlled by landsliding, by seepage erosion, or by overland flow [*Montgomery and Dietrich*, 1989]. This study focuses on the latter process.

The landscape evolution model described below is used to simulate drainage basin response in each of several different climate change scenarios. These scenarios explore changes in the amount and variability of runoff, and in the critical shear stress required for sediment transport (as a proxy for changes

in vegetation cover). No single scenario encompasses the entire range of changes in precipitation, runoff, vegetation, and other processes that appear to have accompanied the Quaternary climate cycles in many parts of the world. Rather, the goal is to explore how the drainage basin as a system responds to changes in only one or two controlling variables. The rationale for this approach is that understanding the system's response to change in a single variable is a prerequisite to understanding the coupled response. Furthermore, there exist potential climate change scenarios in which only one or two factors would be expected to change significantly. The experiments reported herein are offered as a contribution toward the development of a testable, quantitative, process-based theory that can provide a guide to interpreting field observations as well as a guide to predicting the impact of future climate change.

Background

Numerous investigators have attempted to correlate observed changes in Quaternary fluvial systems with known or inferred changes in climate. In particular, much attention has been devoted to unraveling the relationship between climate change and the record of periodic stream aggradation and erosion. Given the complexity of the geomorphic system, it is perhaps not surprising that different studies of fluvial response to climate change often appear contradictory (see, e.g., reviews by *Knox* [1983], *Goudie* [1990], and *Bloom* [1991]). The debate over the geomorphic consequences of climate and land-use change is exemplified by the contrasting models postulated by *Huntington* [1914] and by *Bryan* [1928, 1940]. In what later became known as "Huntington's Principle," [*Fairbridge*, 1968], *Huntington* [1914] proposed that increasing aridity should lead to a loss of vegetation cover, resulting in channel aggradation due to an increase in the sediment flux from side slopes. Incision would occur during more humid periods, when vegetation stabilizes the hillslopes, reducing runoff, peak discharge, and sediment supply. On the other hand, *Bryan* [1928, 1940] argued that greater storm runoff due to a loss of vegetation during arid periods should lead to channel entrenchment rather than to aggradation. Aggradation, in Bryan's view, would instead occur during a transition toward cooler and more humid conditions, as stream energy was reduced.

Field data exist to support both of these hypotheses in different regions of the world. For example, warm-arid aggradation and/or cool-wet entrenchment have been observed or inferred for a number of midlatitude United States and European rivers [e.g., *Brakenridge*, 1980; *Knox*, 1983] and for rivers and gullies in the Niger River basin [*Smith*, 1982]. On the other hand, cool-humid aggradation and/or warm-arid entrenchment have been observed or inferred for arroyos in the American southwest [*Antevs*, 1952; *Leopold*, 1951, 1976], for valleys in the Mediterranean region [*Vita-Finzi*, 1969], for southern Great Plains rivers [e.g., *Blum and Valastro*, 1989], and for Death Valley alluvial fans [e.g., *Dorn*, 1994]. Given these conflicting observations, it is difficult to generalize about how any given drainage basin will respond to changes in climate or land use.

Some of the discrepancies between these observations must reflect differences in vegetation cover, soils, and relief at the time that a climate or land-use change occurs [*Langbein and Schumm*, 1958; *Schumm*, 1977; *Knox*, 1983]. Yet even in the simple case in which vegetation and other factors remained constant, it would be difficult to judge on the basis of intuition

alone how a catchment might respond to an independent change in a single climatic variable, such as precipitation. Suppose, for example, that a watershed experienced an increase in the frequency of large storms without any change in vegetation cover. Would the channels experience incision or aggradation? On the one hand, more stream energy would be available to transport sediment, suggesting that channel incision should result. On the other hand, an increase in storminess might lead to an upslope extension of the channel network with an attendant increase in sediment supply, leading to aggradation. The latter process might be particularly important if, as has been suggested [*Horton*, 1945; *Montgomery and Dietrich*, 1992], the location of channel heads were governed by a threshold of erosion by overland flow.
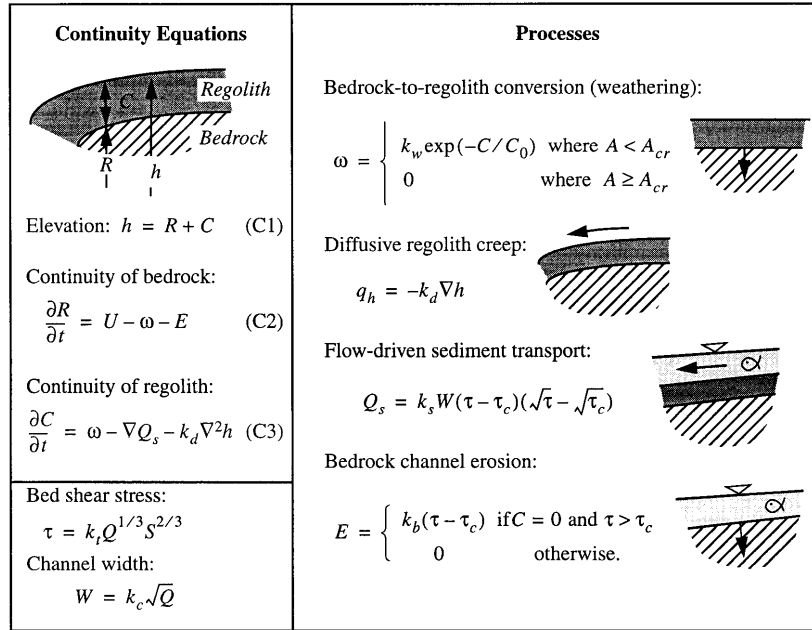
Willgoose [1994] analyzed the response of a transport-limited catchment evolution model to time-varying uplift and climate. For a catchment that is in a quasi-steady state with respect to long-term mean uplift and climate, the model predicts that cyclic variations in runoff will produce an alternation between a state of dynamic equilibrium and a state of "declining characteristic form," with the latter being a quasi-equilibrium state in which relief steadily declines. The primary morphologic difference between these two theoretical states is in the distribution of channel slopes: in the declining relief case, the higher slopes are weighted more toward the higher-elevation parts of a catchment. Thus one prediction of this model is that an increase in runoff in a steady state basin should shift the basin from a state of dynamic equilibrium to a state of declining relief. Such a shift would produce the greatest amount of erosion in the lower portions of the basin. This analysis did not, however, consider the coupling between hillslope and channel processes or the existence of thresholds for sediment movement and channelization.

Rinaldo et al. [1995] modeled the landscape response to sinusoidal climate variations using a "threshold-limited" model. In this model, fluvial erosion is represented by a simple shear-stress threshold algorithm in which landscape pixels are iteratively subjected to "landslides" that instantly reduce the pixel elevation to the threshold level. Dry periods were equated with a high critical shear stress, while wet periods were equated with a low critical shear stress (although, presumably, changes in vegetation might produce the opposite effect, as discussed below). Valley aggradation in the *Rinaldo et al.* [1995] model occurs during times of transition to "arid" conditions (increasing critical shear stress) because the channel network retreats. However, because the *Rinaldo et al.* [1995] model does not account for fluvial deposition (only hillslope processes are capable of redeposition), their results do not directly address the question of how climate change alters the balance between sediment supply and sediment transport capacity within the river network.

Modeling Approach

Our approach to the problem is to analyze the response of an idealized, steady state drainage basin to perturbations in one or more climatically sensitive parameters. To this end, a steady state basin, in which erosion and uplift are everywhere in balance, is used as an initial condition. The parameters for the steady state simulation are chosen such that the properties of the resulting basin, including relief and valley density, approximate those of a 7-km^2 study catchment in the Pennsylvania valley-and-ridge province (called WE-38 hereafter). Such a

**Summary of the Landscape Evolution Model**

Continuity Equations	**Processes**

Elevation: $h = R + C$ (C1)

Continuity of bedrock:

$$\frac{\partial R}{\partial t} = U - \omega - E \qquad (C2)$$

Continuity of regolith:

$$\frac{\partial C}{\partial t} = \omega - \nabla Q_s - k_d \nabla^2 h \quad (C3)$$

Bed shear stress:

$$\tau = k_t Q^{1/3} S^{2/3}$$

Channel width:

$$W = k_c \sqrt{Q}$$

Bedrock-to-regolith conversion (weathering):

$$\omega = \begin{cases} k_w \exp(-C/C_0) & \text{where } A < A_{cr} \\ 0 & \text{where } A \geq A_{cr} \end{cases}$$

Diffusive regolith creep:

$$q_h = -k_d \nabla h$$

Flow-driven sediment transport:

$$Q_s = k_s W(\tau - \tau_c)(\sqrt{\tau} - \sqrt{\tau_c})$$

Bedrock channel erosion:

$$E = \begin{cases} k_b(\tau - \tau_c) & \text{if } C = 0 \text{ and } \tau > \tau_c \\ 0 & \text{otherwise.} \end{cases}$$

Figure 1. Summary of the model used in this study. In the equations, h is elevation, C is regolith thickness, R is the elevation of the bedrock surface, U is tectonic uplift rate, ω is the lowering rate of the bedrock surface due to weathering, q_h is hillslope sediment transport rate per unit slope width, Q_s is volumetric overland or channelized sediment transport rate, τ is shear stress, τ_c is critical shear stress for flow erosion, E is bedrock channel incision rate, Q is water discharge, and S is downslope gradient. C_0, k_w, k_d, k_s, k_b, k_t, and k_c are constants.

scaling exercise is not essential to the problem at hand, but it does provide a set of geologically reasonable parameters as a point of departure.

The model employed in this study is a variant of the GO-LEM landscape evolution model [*Tucker and Slingerland*, 1994, 1996; *Tucker*, 1996]. Four geomorphic processes are represented in the model: (1) the production of regolith from bedrock by mechanical and chemical weathering; (2) sediment transport by hillslope processes such as soil creep; (3) transport of sediment by flowing water; and (4) channel incision into bedrock (Figures 1 and 2). The mathematical representation of

each of these processes is described below. This set of processes is obviously not exhaustive, but it incorporates what we believe to be the most important landscape-forming processes in low- to moderate-relief basins that are dominated by physical rather than chemical erosion. An important advance over previous approaches is the explicit treatment of regolith production. Most previous catchment-scale (as opposed to slope-scale) models assume that ample sediment is always available for transport on a hillslope. By relaxing that assumption, we are able to address important nonlinear effects that result from complete removal of the sediment cover.
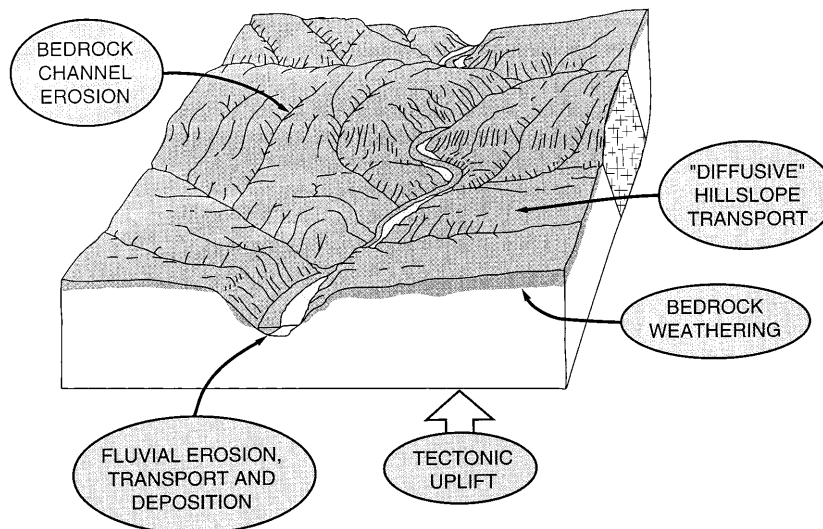
Figure 2. Conceptual illustration of processes incorporated in the model. (Adapted from *Strahler and Strahler* [1978]. Copyright by John Wiley and Sons, Inc.; reprinted with permission.)

An earlier version of the model has been compared with experimental studies and has been shown to reproduce the observed exponential decline in sediment yield following base level lowering [see *Slingerland et al.*, 1993, chap. 3]. The model also reproduces the well-known slope-area scaling relationship for river networks [see *Tucker*, 1996].

Landscape Materials

The model differentiates between bedrock (R) and regolith (C), with the latter being broadly defined as any loosely consolidated granular material (e.g., soil, colluvium, or alluvium) (Figure 1). The thickness of the regolith layer can vary throughout the drainage basin and through time and may be zero (meaning that the bedrock surface is exposed at that point). Bedrock is converted to regolith through weathering or through bedrock stream-channel erosion (see below). Once created, regolith may be transported by hillslope processes or by channelized flow (Figure 1).

Regolith Production

A number of previous models [*Ahnert*, 1976; *Armstrong*, 1976; *Anderson and Humphrey*, 1990; *Rosenbloom and Anderson*, 1994] have assumed that the rate of bedrock-to-regolith conversion by mechanical and chemical weathering is inversely proportional to the thickness of the regolith cover, according to

$$\omega = k_w \exp\left(-C/C_*\right). \tag{1}$$

Here, ω is the vertical rate of descent of a weathering front, k_w is the weathering descent rate for bare bedrock (i.e., $C = 0$), and C_* is a parameter that describes the rate at which the weathering rate decays with increasing regolith thickness (it is the e-folding depth for weathering rate) (Figure 1). Support for this equation comes from a study by *Dietrich et al.* [1995], who modeled steady state colluvial soil thicknesses on creep-dominated hillsides in a northern California watershed. They found that predicted colluvial soil depths correlated well with observed soil depths when regolith production was modeled using (1). Use of a more complex function in which soil production initially increased with increasing soil depth (presumably owing to a greater ability to retain groundwater and sustain vegetation) resulted in a poorer fit. Equation (1) is therefore used in this study to model the bedrock-to-regolith conversion rate on hillslopes.

Some consideration needs to be given to the way in which regolith production is treated in "hillslope" versus "channel" elements of the landscape. Depending on the climate and geology, midlatitude soil-mantled hillslopes are typically subject to both chemical weathering and mechanical weathering by such processes as bioturbation, freeze-thaw, and clay shrinkage and swelling [e.g., *Ollier*, 1984]. However, outside of karst environments, such weathering processes are arguably inactive, or at least much less active, along the beds of perennial stream channels. In perennial channels the presence of flowing water year-round typically prevents the establishment of vegetation and at least partly insulates the bed against freezing. This contention is supported by the observation that in landscapes of moderate relief, hillslopes are often soil-mantled while channels lie on or close to bedrock. Thus it is reasonable to assume for modeling purposes that hillslopes are subject to weathering processes while perennial channels are not. In the present study a perennial channel is assumed to exist in the

model wherever drainage area exceeds a specified threshold value (Figure 1). Equation (1) is not applied to model grid cells that have a contributing drainage area larger than this value, so that lowering of the bedrock surface at these locations can occur only by bedrock channel erosion. Channelized flow may still transport sediment on hillsides or in gullies outside of permanent channels as long as the critical shear stress is exceeded. Such cases represent low-order ephemeral channels that are dry during most of the year.

Hillslope Sediment Transport

Sediment transport by soil creep and related nonconcentrative hillslope processes is modeled as a diffusion process (Figure 1),

$$\left.\frac{\partial h}{\partial t}\right|_{\text{diffusion}} = k_d \nabla^2 h. \tag{2}$$

The use of a diffusive transport law is supported by a number of studies of scarp degradation [*Nash*, 1980; *Colman and Watson*, 1983; *Hanks et al.*, 1984; *Rosenbloom and Anderson*, 1994] as well as by two recent studies in which concentrations of atmospherically produced radionuclides were used to estimate mass movement rates along a hillslope profile [*Monaghan et al.*, 1992; *McKean et al.*, 1993].

Flow-Driven Sediment Transport

A critical question in this study concerns the role of a threshold of erosion by surface flow. From laboratory, field, and theoretical studies of sediment transport mechanics it is well known that transport of sediment grains by free-surface flow does not occur until a threshold of flow strength is exceeded [e.g., *Yalin*, 1977]. More recently, studies of watersheds in the western United States support the theory originally proposed by *Horton* [1945], that a similar erosion threshold also controls the location of channel heads in some drainage basins [*Montgomery and Dietrich*, 1989; *Dietrich et al.*, 1993]. These studies suggest that channels form where the shear stress generated by surface flow during storms is just large enough to break through the vegetation mat to entrain and transport sediment particles. If this hypothesis is correct, then the extent of the channel network should be especially sensitive to changes in climate [*Montgomery and Dietrich*, 1992]. If, for example, an increase in storm magnitude or frequency raises overland flow shear stresses, then drainage density will increase and more sediment will be delivered to the main channel network, possibly leading to aggradation.

In order to model this type of erosion threshold, a critical shear stress for particle entrainment and channel initiation is included in the fluvial sediment-transport equation. Sediment transport by overland and channelized flow is modeled using a variant of the Bagnold bedload equation [*Bridge and Dominic*, 1984; *Slingerland et al.*, 1993]. Phrased in terms of total volumetric transport rate, Q_s, the equation is

$$Q_s = \frac{W a_t}{(\sigma - \rho)\rho^{1/2} g}\left(\tau - \tau_c\right)\left(\tau^{1/2} - \tau_c^{1/2}\right), \tag{3}$$

where τ is bed shear stress, τ_c is the critical shear stress for particle entrainment, W is channel width, g is gravitational acceleration, a_t is a dimensionless constant, and σ and ρ are the densities of sediment and water, respectively. Although this is a bed load rather than a total-load equation, its predicted cubic dependence on cross-sectional average flow velocity is

consistent with total-load formulas, which typically predict between a 3rd and a 4th power dependence on velocity [*Graf*, 1971; *Yang*, 1996].

Bed shear stress, τ, can be related to channel gradient and discharge by combining several well-known hydraulic relationships:

Steady, uniform flow:

$$\tau = \rho g R S \qquad (4)$$

Wide channels:

$$R \cong d \qquad (5)$$

Continuity of mass:

$$Q = VWd \qquad (6)$$

Darcy-Weisbach equation:

$$V = \left(\frac{8gRS}{f}\right)^{1/2} \qquad (7)$$

where ρ is water density, g is gravitational acceleration, R is hydraulic radius, d is channel depth, W is channel width, V is mean flow velocity, and f is a dimensionless friction factor [*Yalin*, 1977]. Combining (4)–(7) gives

$$\tau = \frac{\rho g^{2/3} f^{1/3}}{2}\left(\frac{Q}{W}\right)^{2/3} S^{2/3}. \qquad (8)$$

Empirically, channel width, W, is known to vary with discharge as a power law,

$$W = k_c Q^{m_c}, \qquad (9)$$

with m_c being on the order of 1/2 and showing remarkably little variation among different rivers [*Yalin*, 1992]. Here, Q represents the steady runoff rate produced by the "dominant" storm, as discussed below. For notational convenience the constants can be lumped into two terms:

$$a = \frac{a_t k_c}{(\sigma - \rho)\rho^{1/2} g} \qquad (10)$$

and

$$\delta = \frac{\rho g^{2/3} f^{1/3}}{2 k_c^{2/3}}. \qquad (11)$$

Substituting (8)–(11) into the sediment transport equation (equation (3)) gives

$$Q_s = aQ^{1/2}(\delta Q^{1/3} S^{2/3} - \delta[Q^{1/3} S^{2/3}]_c)$$
$$\cdot \{(\delta Q^{1/3} S^{2/3})^{1/2} - (\delta[Q^{1/3} S^{2/3}]_c)^{1/2}\} \qquad (12)$$

with the subscript c indicating a critical threshold discharge-slope quantity. Collecting terms, and denoting the threshold discharge-slope quantity as Φ_c for convenience, the sediment transport capacity is

$$Q_s = k_f Q^{1/2}(Q^{1/3} S^{2/3} - \Phi_c)[(Q^{1/3} S^{2/3})^{1/2} - (\Phi_c)^{1/2}] \qquad (13)$$

where the transport efficiency coefficient k_f equals $a\delta^{3/2}$. The meaning of the discharge term Q in the context of climate change is discussed below. For the sake of simplicity, no distinction is made between the threshold necessary to create a new channel by disrupting vegetation, and that required to entrain sediment grains within an established channel.

Channel Incision Into Bedrock

Active channel incision into bedrock is presumed to occur wherever the local sediment transport capacity is greater than the available supply [*Gilbert*, 1877; *Montgomery et al.*, 1996]. It has been suggested that in some settings the rate of channel erosion into bedrock is proportional to bed shear stress (or some power thereof) [*Howard and Kerby*, 1983; *Howard*, 1994]. Such a relationship is supported by a field study of channel incision into badlands [*Howard and Kerby*, 1983]. It is also consistent with the observation of a power law relationship between channel gradient and drainage area in natural river basins,

$$S \propto A^{-\theta}, \qquad (14)$$

with the area exponent typically equal to about 0.5 [e.g., *Flint*, 1974; *Tarboton et al.*, 1989]. This power law relationship holds true for the WE-38 catchment that is used as the basis for model scaling in the present study, with $\theta \cong 0.45$ for the catchment itself and $\theta \cong 0.49$ for the larger basin in which it is embedded [*Tucker*, 1996]. These data provide support for the assumption that the rate of channel incision into bedrock is proportional to bed shear stress. Here, we assume the dependence is linear [*Howard and Kerby*, 1983] and given by

$$\left.\frac{\partial h_b}{\partial t}\right|_{\text{bedrock}} = -k_t(\tau - \tau_c), \qquad (15)$$

where h_b is channel elevation relative to a datum within the underlying rock column, and k_t is a proportionality constant. Equation (15) can be recast in terms of discharge and slope by substituting (8) for the shear stress terms and (9) for channel width, which gives

$$\left.\frac{\partial h_b}{\partial t}\right|_{\text{bedrock}} = -k_b(Q^{1/3} S^{2/3} - \Phi_c), \qquad (16)$$

where the bedrock erodibility coefficient, k_b, is equal to δk_t. For lack of a better constraint, the erosion threshold Φ_c is assumed to be the same for both sediment entrainment and the initiation of bedrock-channel scour. This treatment is based partly on the assumption that channel scour will not occur until grains on the bed have been mobilized.

Treatment of Hydrology

The sediment transport rates computed by the model are considered to be averages over tens to hundreds of years. It is necessary, therefore, to define what "average" discharge means in this context. *Willgoose* [1989] derived an analytical formula for long-term transport rates by assuming typical flood frequency curves and a generic sediment transport formula of the form $q_s \propto q^m S^n$, and he showed that mean peak discharge is an appropriate average quantity. Here, we take a simpler approach that has the added advantage of allowing for a transport threshold, a variable not considered in *Willgoose*'s [1989] analysis. Consider the simple case of a drainage basin in which geomorphic evolution is dominated by flood events of a single characteristic size and recurrence interval. If we assume that precipitation, runoff, and channel discharge are steady throughout each storm event, and if we further assume that discharge is linearly related to drainage area (in other words, equal to the product of runoff rate and drainage area), then (13) can be used to describe the instantaneous sediment transport rate, with the discharge term given by
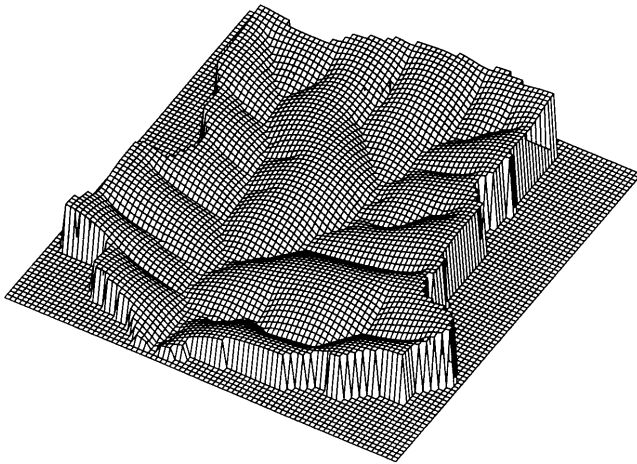
Figure 3. Equilibrium drainage basin used as an initial condition. Basin configuration is that of the WE-38 watershed, a 7-km^2 watershed in central Pennsylvania, United States.

$$Q = P_s A, \tag{17}$$

where P_s is the storm runoff rate per unit area. In order to relate these instantaneous quantities to long-term averages, a "total flood duration ratio," $\mathcal{F}$, is defined as the total fraction of a given year that the drainage basin is subject to flooding. For example, if rainfall occurred continually at a uniform rate throughout the year, $\mathcal{F}$ would equal 1, whereas if all of the annual runoff-producing rainfall fell during one day, $\mathcal{F}$ would equal 1/365. The instantaneous storm runoff rate can then be related to the mean annual runoff rate, $\bar{P}_e$, by

$$P_s = \frac{\bar{P}_e}{\mathcal{F}}. \tag{18}$$

The mean annual sediment transport rate in a channel, $\bar{Q}_s$, is equal to the instantaneous transport rate times the fraction of the year that the channel experiences that transport rate,

$$\bar{Q}_s = Q_s \mathcal{F}. \tag{19}$$

This equation simply says that the same mean annual runoff may be generated by frequent (or long-lasting) gentle runoff events (low P_s, high $\mathcal{F}$) or by infrequent (or short-lived) intense runoff events (high P_s, low $\mathcal{F}$). Given that sediment transport is a nonlinear function of Q when τ is close to τ_c, changes in event magnitude and frequency may be expected to have a significant impact on erosion and deposition within a threshold-dominated drainage basin. Where the assumption that channel network extent is controlled by a shear stress

threshold holds true, drainage density and sediment transport may be particularly sensitive to changes in event magnitude and frequency. This sensitivity is explored in the simulations that follow.

Initial and Boundary Conditions

In order to model the effects of climatic perturbation, an idealized steady state catchment is used as an initial condition (Figure 3). The properties of this catchment, including size, shape, and drainage pattern, are based upon those of the WE-38 watershed, a 7.2-km^2 catchment that is part of the Susquehanna River drainage basin in central Pennsylvania, United States [*Tucker*, 1996]. Model parameters were chosen such that the simulated catchment resembles the study area in terms of valley and channel density, overall relief, and the slope/area relationship in the main channels (Table 1). This calibration exercise is, of necessity, inexact. Long computation times render proper inverse modeling impractical, and given the uncertainty in the Quaternary geomorphology of this watershed, such an exercise is in any event unwarranted. The point, rather, is to place the simulations within a geologically reasonable framework.

The outlet point at the base of the catchment is held at a fixed elevation through time, and any sediment reaching this point is assumed to be transported away. The remaining edges of the catchment are treated as no-flux boundaries. The model catchment is initially subjected to steady, uniform tectonic uplift until a state of equilibrium between uplift and denudation is reached. A series of numerical experiments is then conducted in which the steady state landscape is subjected to changes in mean annual runoff ($\bar{P}$), runoff intensity (P_s), or the critical shear stress for channelization (τ_c). The use of a steady state initial catchment guarantees that any observed changes are the direct result of change in the environmental variable, rather than the result of an initial landscape disequilibrium.

Results

Nine different scenarios are considered in the climate perturbation analysis (Table 2). Five of these explore the effect of instantaneous perturbations in storm frequency and magnitude, or in Φ_c. Four others consider longer-term cyclic forcing in runoff intensity, with change being either smoothly varying (sinusoidal) or sudden (stepped) in nature. The experiments are summarized in Table 2.

A Note on Timescales

Although the various parameters are scaled to an assumed steady rate of uplift and thus imply meaningful timescales,

Table 1. Parameters Used in the Initial Equilibrium Simulation

Description	Parameter	Value	Equation
Grid size	$\cdots$	82 by 87 cells	$\cdots$
Cell size	Δx	40 m	$\cdots$
Bedrock erodibility	k_b	6×10^{-5} yr$^{-2/3}$	(16)
Sediment transport efficiency	k_f	1.0	(13)
Erosion threshold value	Φ_c	10 m yr$^{-1/3}$	(13)
Runoff rate	P_s	1 m yr^{-1}	(17)
Bare bedrock sediment production rate	k_w	0.0005 m yr^{-1}	(1)
Sediment production decay constant	m_w	0.5 m	(1)
Hillslope diffusivity coefficient	k_d	0.01 m^2 yr^{-1}	(2)
Tectonic uplift rate	U	10^{-5} m yr^{-1}	(C2)

Table 2. Summary of the Climate Perturbation Experiments

Scenario	Description	$\Delta \bar{P}$*	ΔP_s†	$\Delta \mathcal{I}$‡	$\Delta \Phi_c$§
1	increase in storm frequency (wetter)	4 ×	1 ×	4 ×	⋯
2	decrease in storm frequency (drier)	0.25 ×	1 ×	0.25 ×	⋯
3	decrease in runoff intensity	1 ×	0.25 ×	4 ×	⋯
4	increase in runoff intensity	1 ×	4 ×	0.25 ×	⋯
5	decrease in surface resistance (corresponding to vegetation loss)	⋯	⋯	⋯	0.5 ×
6	sinusoidal variation in runoff intensity (short period)	1 ×	0.5–1.5 ×	0.5–1.5 ×	⋯
7	sinusoidal variation in runoff intensity (long period)	1 ×	0.5–1.5 ×	0.5–1.5 ×	⋯
8	step variation in runoff intensity (short period)	1 ×	0.5–1.5 ×	0.5–1.5 ×	⋯
9	step variation in runoff intensity (long period)	1 ×	0.5–1.5 ×	0.5–1.5 ×	⋯

*Change in mean annual runoff, relative to control run.
†Change in storm runoff rate per unit area, relative to control run.
‡Change in total flood duration ratio, relative to control run.
§Change in erosion threshold value, relative to control run.

uncertainty in these timescales remains, due both to uncertainty in the estimated long-term uplift rate [*Pazzaglia and Gardner*, 1994] and, more importantly, to uncertainty in the calibration catchment's Quaternary geomorphic history. Thus the absolute time values in the simulations are less meaningful than the relative differences in timescale between the different simulations. Time in the simulations can be expressed in dimensionless form as

$$T_* = \frac{TU}{R}, \qquad (20)$$

where T_* is nondimensional time, T is elapsed time in model years, U is the steady tectonic uplift rate, and R is the basin's total relief at steady state.

Changes in Storm Frequency or Duration

The effects of an increase in runoff frequency and/or duration are shown in Figures 4 and 5. This represents a scenario in which the climate becomes more humid without any change in the average storm size (scenario 1, Table 2). Because the runoff intensity does not change, the extent of the channel network remains essentially stable (Figure 4). In each element of the landscape that is subject to flow-driven erosion (that is, wherever $\tau > \tau_c$), there is a competition between flow-driven erosion, which tends to carve channels, and diffusive transport, which tends to fill them in. The balance between these two processes is most delicate near channel heads. Thus, in the simulation pictured in Figure 4, one result of the increase in the rate of flow-driven erosion is accelerated excavation at the tips of the valley network. Over time, the increase in mean runoff also leads to accelerated bedrock scour along the main channel network (Figure 4b). Compared with scenarios in which runoff intensity rather than duration increases, the response time in this scenario is quite long.

A decrease in storm frequency and/or duration (Figures 6 and 7) likewise alters the balance between hillslope and channel transport rates. With the sediment transport capacity along the fluvial system reduced, channels undergo slow aggradation. The aggradation rate is initially greatest near the catchment

outlet. Note the disappearance of several small, first-order channels between the two time slices shown in Figure 6. As noted elsewhere, channel heads are especially sensitive to changes in the balance between hillslope and fluvial processes. In this example, some of the smaller first-order channels are no longer able to remove sediment as fast as it is being fed in from the adjoining side-slopes, and therefore they begin to fill with sediment.

The origin of the downstream increase in channel aggradation rate arises from the transition from bedrock channels to alluvial channels. The sediment transport equation (equation (3)) describes alluvial channel longitudinal profiles that tend to be less concave than their bedrock counterparts, which are described by (15) [see also *Howard*, 1994]. For an equilibrium channel network initially composed of concave bedrock channels, the sediment transport capacity (via (3)) increases downstream less rapidly than does sediment supply. As an illustration, imagine that the slope along a bedrock channel network initially decreases as a power law with increasing drainage area, as $S \propto A^{-p}$. The power law exponent p is equal to about 1/2 for many basins (including the Pennsylvania study site mentioned earlier), and it is that value toward which the bedrock erosion equation (equation (15)) will tend. If the erosion rate is roughly uniform across the catchment, then the total sediment flux will increase linearly with drainage area (Figure 8). By (3), however, sediment-carrying capacity will increase with area less than linearly because the increase in flow is partly offset by a reduction in gradient. (This is so because the transport equation (equation (3)) is nearly linear in both gradient and discharge.) At some point downstream the sediment supply becomes equal to the carrying capacity. This marks the bedrock-alluvial transition. If transport capacity were reduced, for example, owing to a reduction in storm frequency, the bedrock-alluvial transition point would shift upstream, leading to channel aggradation. Since the degree of departure from the new, less concave alluvial equilibrium profile would increase downstream, so too would the aggradation rate (at least initially) increase downstream. This is why, in Figure 6, aggradation appears to propagate upstream through time.
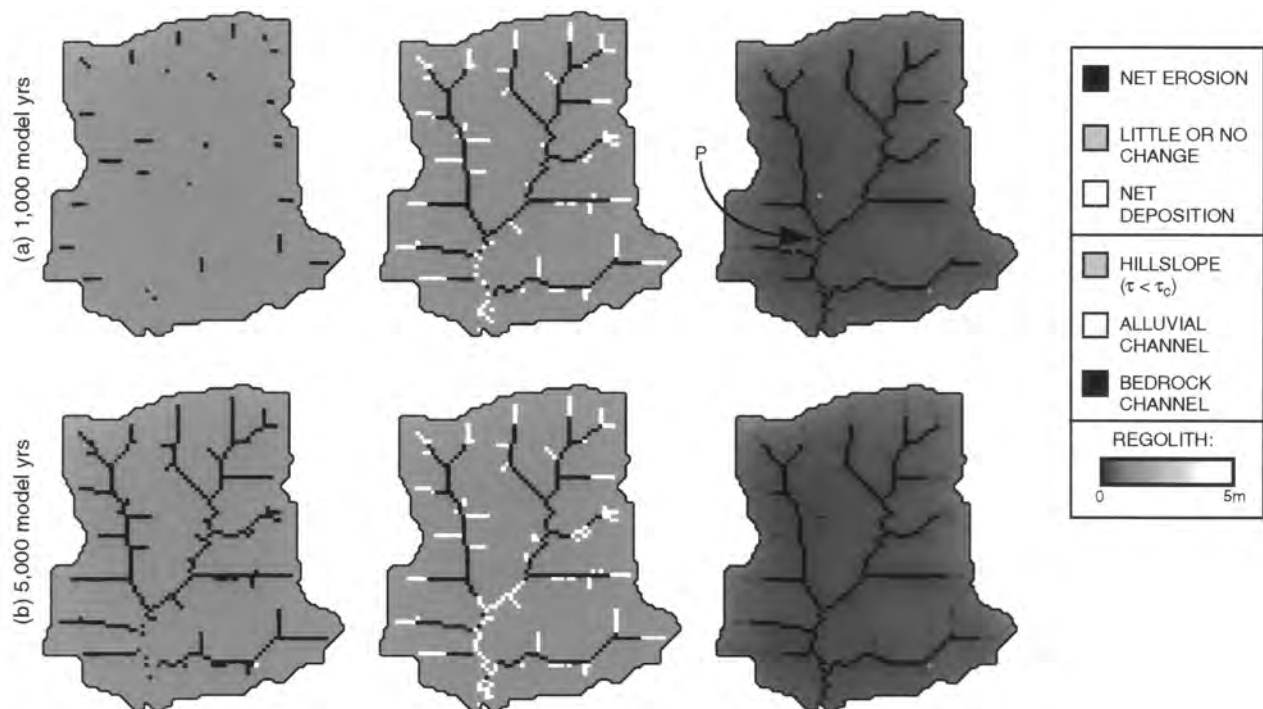
Figure 4. Simulated impact of an increase in the frequency of runoff events with no change in runoff intensity. Maps show cumulative erosion/deposition, distribution of channel types, and regolith thickness at two time slices in the simulation. Locations marked "alluvial channel" are places where sediment transport is active ($\tau > \tau_c$) and regolith is present; those marked "bedrock channel" are locations where fluvial erosion of exposed bedrock is occurring (also $\tau > \tau_c$). Left, middle, and right columns show erosion/deposition, channel network, and regolith thickness, respectively.

Whether such differences in longitudinal-profile concavity between bedrock and alluvial channels do in fact exist remains as an important issue for further study. We do know of at least one data set, however, that appears to support the contention that alluvial depositional profiles are markedly less concave than bedrock erosional profiles [*Sugai*, 1993].

Changes in Runoff Intensity

We next consider changes in runoff intensity, keeping mean annual runoff constant (Table 2, scenarios 3 and 4). These scenarios correspond to changes in storminess with little or no change in mean annual rainfall. With a decrease in runoff
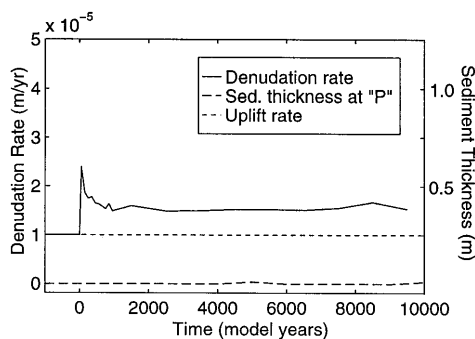
Figure 5. Mean catchment denudation rate, and sediment thickness at a representative point (P on Figure 4) along the channel network, in response to an increase in runoff frequency/duration. Constant tectonic uplift rate is shown for comparison with denudation rate.

intensity (Figures 9 and 10) the effective shear stresses experienced by the catchment during floods are decreased, with the result that the active channel network retreats. In this example the reduction in runoff intensity is large enough that the entire catchment drops below the erosion threshold. Cessation of fluvial sediment transport along the main valley network leads to slow aggradation as material continues to be fed in from side slopes. Because fluvial transport has ceased (unlike the case depicted in Figure 6, in which it continues at a reduced rate), aggradation is uniform throughout the network. Continuing tectonic uplift relative to the fixed outlet point eventually reactivates fluvial sediment transport near the catchment outlet (Figure 9b). Were uplift to continue long enough, a new equilibrium state with a steeper valley network would ultimately develop.

The response to an increase in runoff intensity (Figures 11 and 12) is both much faster and much different in character than the response to a decrease in intensity. The increase in surface shear stress leads to a rapid upslope extension of the channel network. Erosion of the former side slopes leads to a large increase in the sediment flux to the main channel network, resulting in rapid valley aggradation (Figure 11a). Over time, the sediment influx diminishes, due both to a reduction in the gradient of low-order channels and to increasing exposure of bedrock on headwater slopes (Figure 11b). As the sediment flux to the main channel network drops off, sediment previously deposited within the network is progressively remobilized, with erosion propagating downstream through time (Figure 11b). In that sense, the model's geomorphic response is similar to a catchment's hydrologic response, with a sediment "wave" propagating down the branches of the channel network.
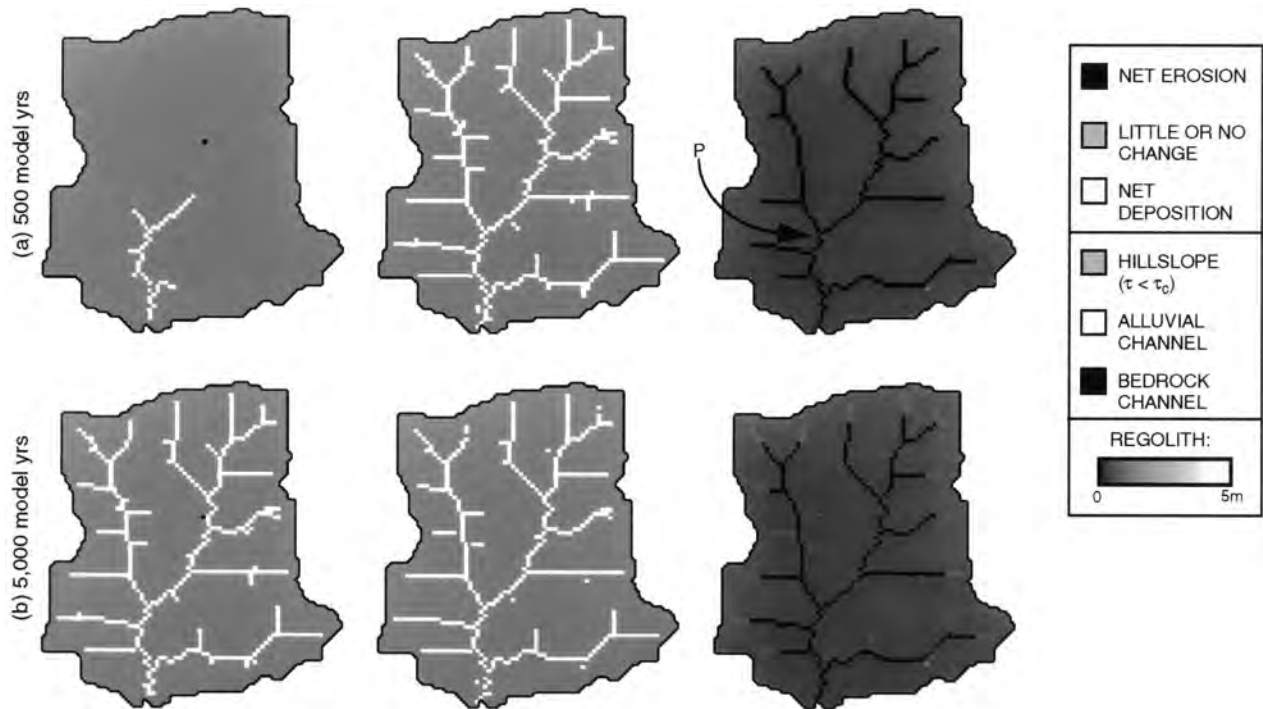
Figure 6. Simulated impact of a decrease in the frequency of runoff events with no change in runoff intensity. Left, middle, and right columns show erosion/deposition, channel network, and regolith thickness, respectively.

This pattern of successive deposition and erosion is reflected in the mean denudation-rate curve and in the sediment thickness at a point along the main channel network (Figure 12). The timescale of response in this scenario is considerably shorter than in the previous two cases (compare Figure 12 with Figures 5 and 7). This suggests the potential for a punctuated response to cyclically varying climate, as explored further below.

Changes in Surface Resistance

One of the most significant controls on catchment sediment yield is vegetation cover [e.g., *Langbein and Schumm*, 1958; *Douglas*, 1967; *Wilson*, 1973]. The parameter Φ_c describes the land surface resistance to erosion by surface flow, and it is a function of both vegetation cover and soil erodibility. Figures 13 and 14 portray the model's response to a two-fold decrease in Φ_c, which might represent, for example, a rapid loss of vegetation. For the sake of simplicity, changes in slope stability that might also result from vegetation loss are not considered.
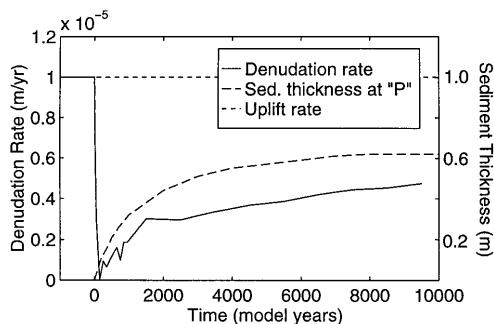
Figure 7. Mean catchment denudation rate and sediment thickness at a representative point (P on Figure 6) along the channel network, in response to a decrease in runoff frequency/duration.

As might be expected, the results (Figure 13) are quite similar to the case in which runoff intensity was increased (Figure 11). The decrease in the erosion threshold leads to a rapid expansion of the channel network onto previously unchanneled hillsides. Rapid erosion on the hillsides delivers more sediment to the main channel network than can be transported, and the channels fill with sediment. As the sediment flux subsequently declines, channels cut down again in a wave of erosion that propagates from upstream to downstream. Isolated remnants of the alluvial or colluvial deposits are left behind as "fill-terrace" fragments (Figure 13b).

Note that the extent of hillside erosion and valley aggradation in this scenario (Figure 13) is greater than was the case in scenario 4 (Figure 11), even though the magnitude of change is less (Table 2). This reflects an especially high sensitivity to changes in the erosion threshold value. Equations (8), (9), and (17) imply that at the point where flow-driven erosion just begins to be initiated (that is, where $\tau = \tau_c$),

$$\tau_c^3 \propto P_s A S^2. \qquad (21)$$

Thus a two-fold change in τ_c (or equivalently in Φ_c) corresponds to an eight-fold change in runoff intensity [cf. *Dietrich et al.*, 1992].

The model's response to an increase in the erosion threshold value (not pictured) is essentially the same as the response to a decrease in runoff intensity (Figure 9). The increased erosion threshold causes the channel network to retreat. Retreat of the channel network is accompanied by slow aggradation in the former channels, just as in scenario 2. Since no distinction is made between the erosion threshold value on hillsides and within permanent channels, a uniform reduction in Φ_c would represent a case in which vegetation was able to colonize even the permanent channels. The more complicated but more realistic case in which the erosion threshold behaves differently on hillsides and in channels remains as an issue for further study.
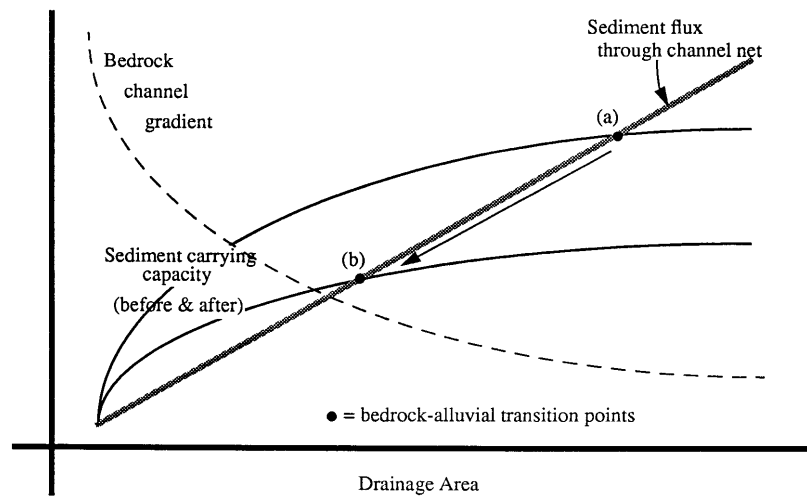
Figure 8. Schematic illustration of the relationship between sediment flux and sediment carrying capacity along a bedrock channel. If the sediment delivery rate per unit area from hillslopes is roughly uniform, and deposition is not occurring, sediment flux will increase linearly with drainage area (gray line). Sediment carrying capacity may increase less than linearly with drainage area because the increase in flow is partly offset by a decrease in gradient. (a) Transition from bedrock (detachment-limited) to alluvial (capacity-limited) channel occurs where the sediment flux reaches the carrying capacity. (b) If the carrying capacity diminishes, for example, owing to a decrease in storm frequency, the transition point will shift upstream, leading to aggradation along the former bedrock reach (see Figure 6).

Longer-Term Cyclic Change

It is also of interest to consider how a drainage basin might respond to repeated changes of the sort associated with Quaternary climate cycles. Of particular importance are responses to cyclic changes in runoff intensity. Regional changes in storm size and frequency are known to have accompanied Quaternary climate oscillations in various parts of the world and have been correlated with episodes of fluvial erosion and deposition [e.g., *Brakenridge*, 1980; *Blum and Valastro*, 1989; *Sugai*, 1993]. Given that many drainage basins around the world have probably been subject to such oscillations, several important questions arise:

1. How are catchment denudation rates distributed in time over the course of a climate cycle?
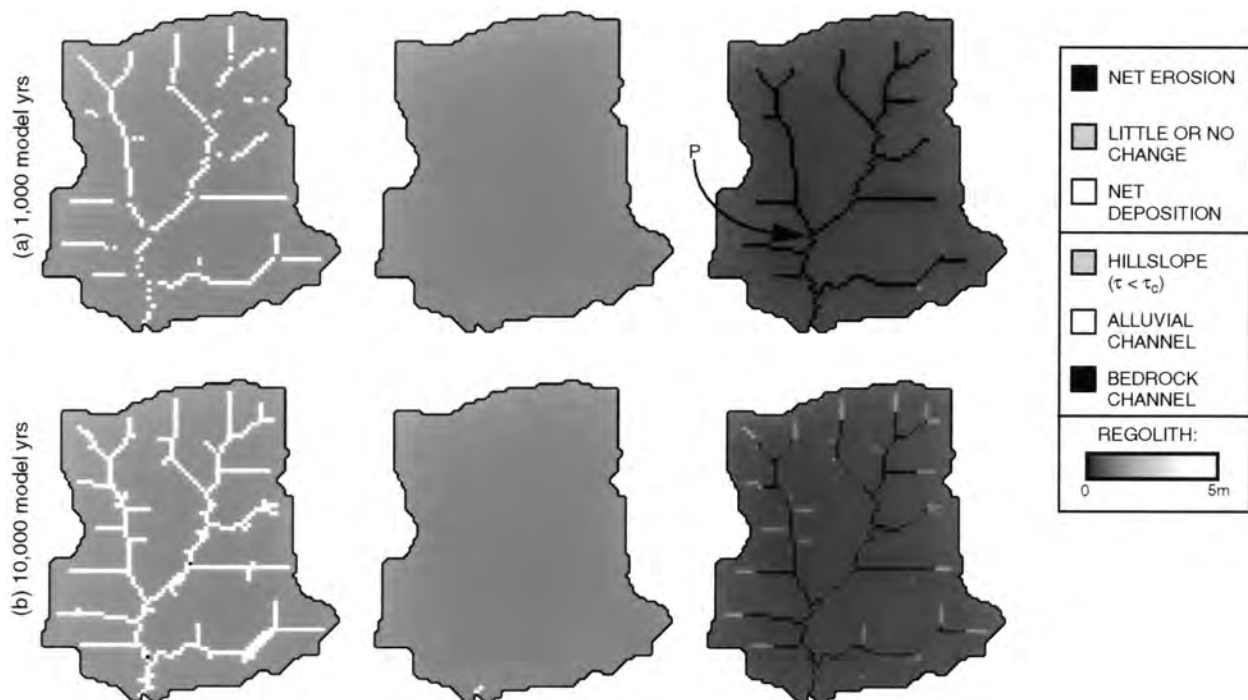
Figure 9. Simulated impact of a decrease in the magnitude of runoff events with no change in mean annual runoff. Note the disappearance of active channels. Left, middle, and right columns show erosion/deposition, channel network, and regolith thickness, respectively.
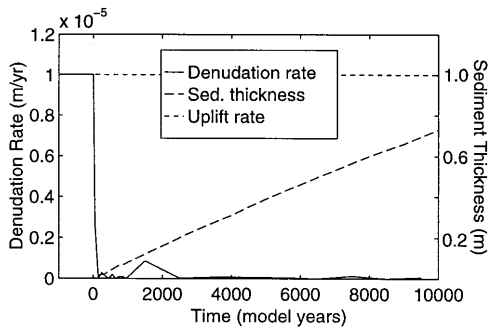
Figure 10. Mean catchment denudation rate and sediment thickness at a representative point (P on Figure 9), in response to a decrease in runoff intensity.
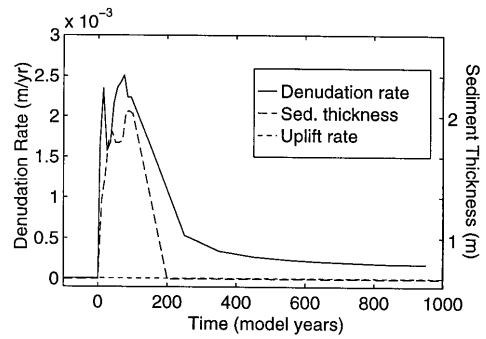
Figure 12. Mean catchment denudation rate and sediment thickness at a representative point along the channel network (P on Figure 11), in response to an increase in runoff intensity. Note the difference in time scale between this and the preceding three simulations (Figures 5, 7, and 10).

2. At what point(s) during a climate cycle are valley erosion and deposition likely to occur?

3. How is a catchment's geomorphic response likely to vary as a function of the timescale of forcing?

4. Does it matter whether climate change is gradual or punctuated?

These issues have obvious implications for interpreting alluvial stratigraphic sequences, as well as for understanding the relationship between past and present denudation rates. They are explored here through four model simulations, two of which involve sinusoidal changes in runoff intensity, and two of which involve repeated step changes in runoff intensity. The latter are motivated in part by the finding from ice-core studies that transitions between climate states can occur very rapidly, on timescales of years to decades [*Alley et al.*, 1993; *Taylor et al.*, 1993]. In each case the mean annual runoff remains constant,

so that the simulations represent changes in storm size with little or no change in overall humidity.

In response to sinusoidal changes in runoff intensity (Figures 15 and 16), catchment denudation rates become highly punctuated in time, with denudation concentrated during the rising limb of the runoff intensity curve. Peak denudation rates occur either near the time of peak runoff (Figure 15) or near the start of the intense runoff period (Figure 16).

If the timescale of climate forcing is short relative to the timescale of basin response, the catchment will have insufficient time to "heal" between periods of rapid denudation. This is why the initial response in the short-period case (Figure 15) differs from the subsequent responses. At the start of the first cycle, a uniformly thick colluvial mantle just upslope of the
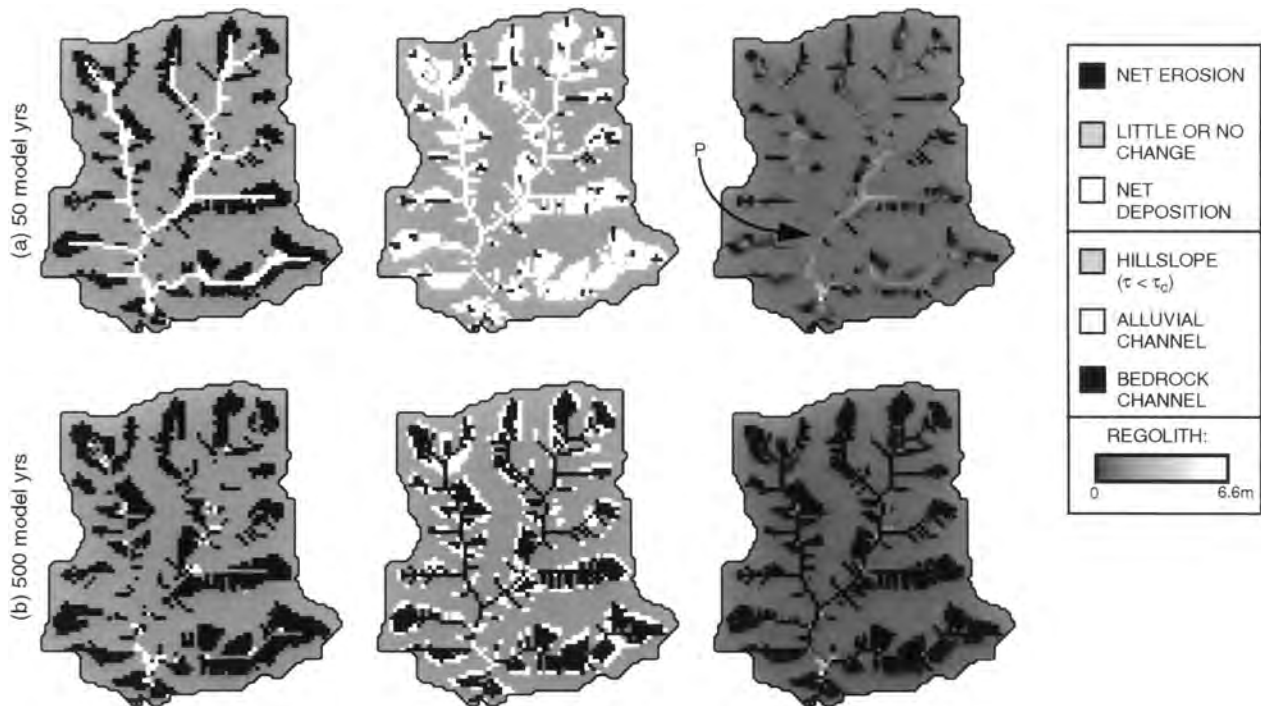
Figure 11. Simulated impact of an increase in the magnitude of runoff events with no change in mean annual runoff. Note the difference in timescales between this and the preceding simulations (Figures 4, 6, and 9). Left, middle, and right columns show erosion/deposition, channel network, and regolith thickness, respectively.
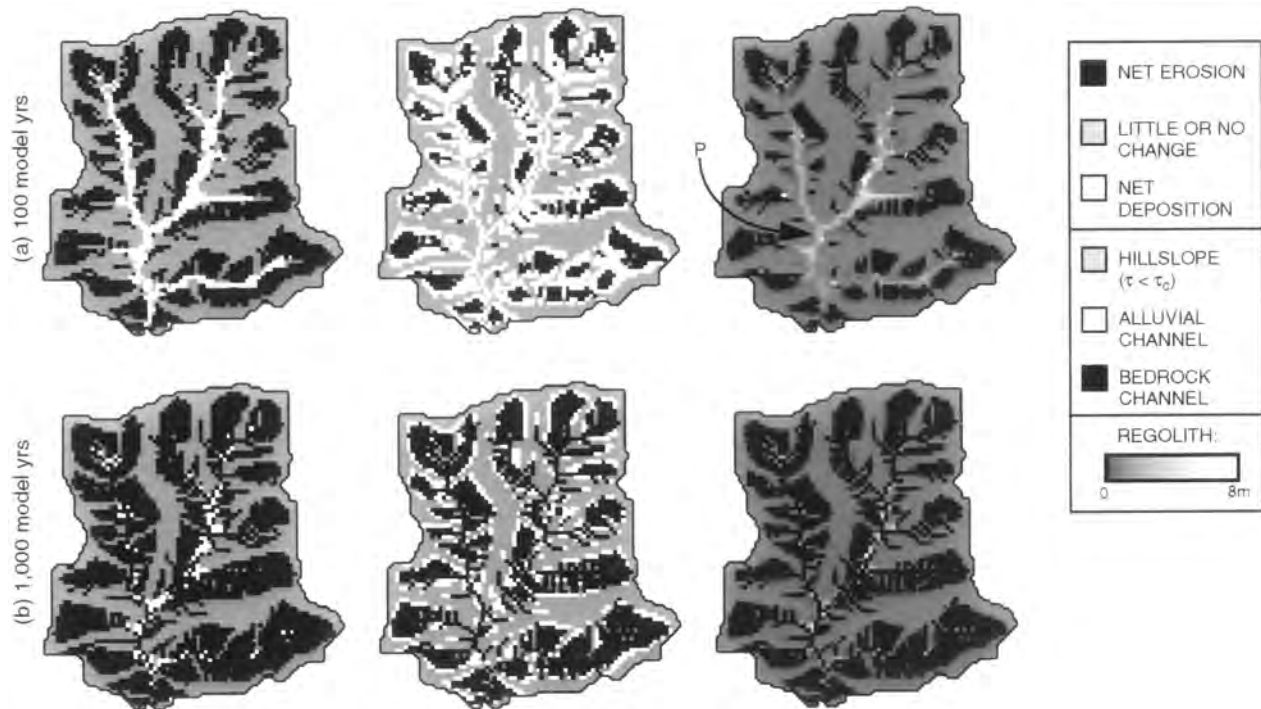
Figure 13. Simulated impact of a two-fold decrease in the erosion threshold (τ_c). The response is similar to the response to an increase in runoff intensity (Figure 11), because both cases involve an increase in the ratio of applied shear stress to critical shear stress. Left, middle, and right columns show erosion/deposition, channel network, and regolith thickness, respectively.
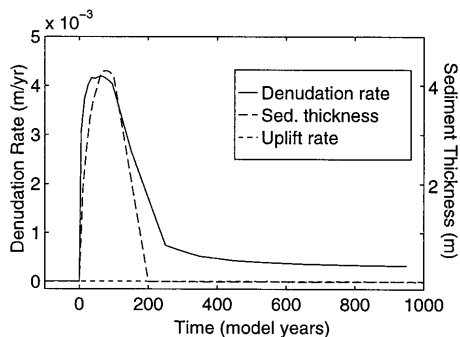
active channel network provides an ample supply of sediment that is evacuated as the network extends headward (just as in Figure 11). During subsequent cycles, however, insufficient time is available to regenerate this sediment mantle in hollows and on lower slopes, leading to a damped response. In this sense the catchment retains a "memory" of earlier conditions. By comparison, such damping does not occur when the timescale of forcing is comparable to the timescale of response (Figure 16).

Sedimentation within the main channel network begins near the inflection point on the descending limb of the runoff intensity cycle (Figures 15 and 16). The depth of aggradation reflects the period of forcing. "Spikes" in the sedimentation rate just prior to the inflection point on the rising limb of the runoff cycle result from rapid sediment evacuation from hol-

lows and lower valley side slopes. This is followed by rapid downcutting as the sediment supply from headwaters diminishes. In the case of longer-period forcing (Figure 16), rapid removal of sediment temporarily stored in the channel network is reflected by a short-lived spike in the mean denudation rate immediately following the inflection point on the rising limb of the runoff curve.

The secondary oscillation in channel alluviation (Figure 16b) appears to reflect a feedback between channels and hillslopes. Rapid downcutting along the channel network produces a local acceleration in the sediment delivery rate from lower slopes and low-order tributaries, leading to a temporary reversal in the process of channel entrenchment.

Abrupt rather than smooth variations in runoff intensity accentuate the punctuated nature of catchment denudation (Figures 17 and 18). Denudation rates are concentrated near the onset of each period of intense runoff. The sequence of rapid channel aggradation followed by erosion discussed earlier (Figure 11) again shows up as short-lived "spikes" of channel sedimentation immediately following the end of each low-intensity runoff episode (Figure 18). In other respects, the model's response to abrupt variations resembles the response to smoother variation.
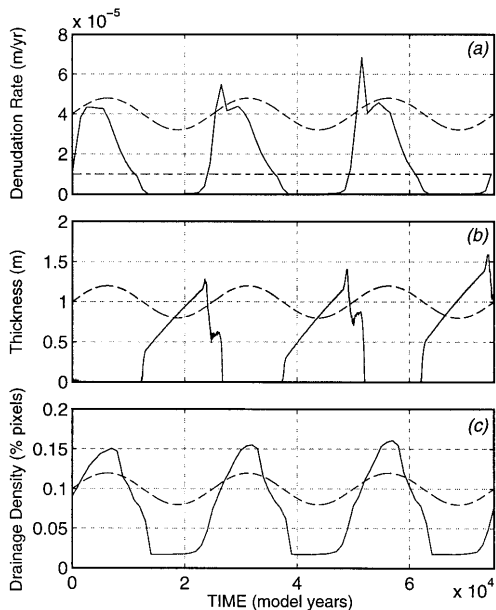
Discussion

These results highlight the sensitivity of a threshold-dominated catchment to changes in runoff intensity and/or surface resistance. Notably, the response time to changes in runoff intensity or in critical shear stress depends on the direction of change. An increase in runoff intensity (storm magnitude) or a decrease in the erosion threshold will both trigger a rapid upslope extension of the channel network, resulting in

Figure 14. Mean catchment denudation rate and sediment thickness at a representative point along the channel network (P on Figure 13), in response to a decrease in the erosion threshold (τ_c).
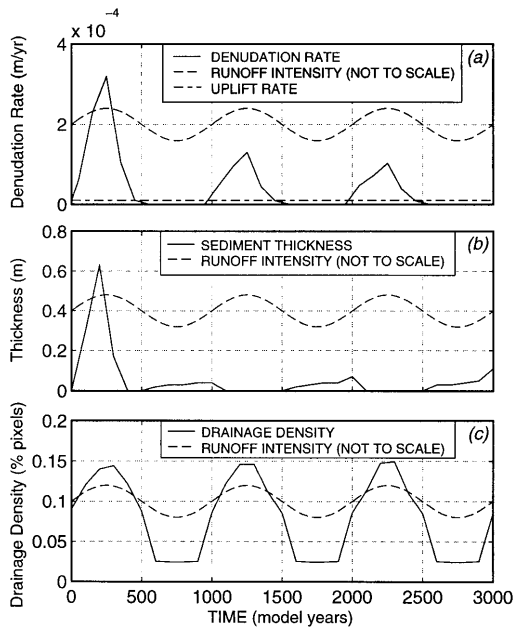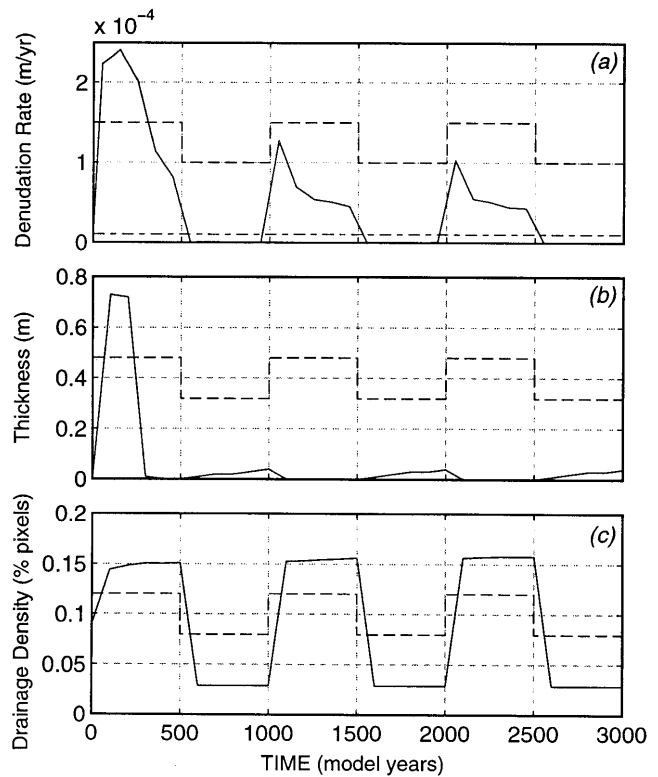
Figure 15. Basin response to short-period sinusoidal variations in runoff intensity (see Table 2). (a) Mean basin denudation rate. (b) Sediment thickness at a representative point along the main channel network. (c) Drainage density, defined as the proportion of model cells in which the erosion threshold is exceeded. Runoff curves are not drawn to scale. Note the difference between the initial and subsequent responses.

rapid evacuation of colluvium from the previously unchanneled lower slopes and hollows. By contrast, the model responds much more slowly to a decrease in storm magnitude or an increase in the erosion threshold, and therefore the effects
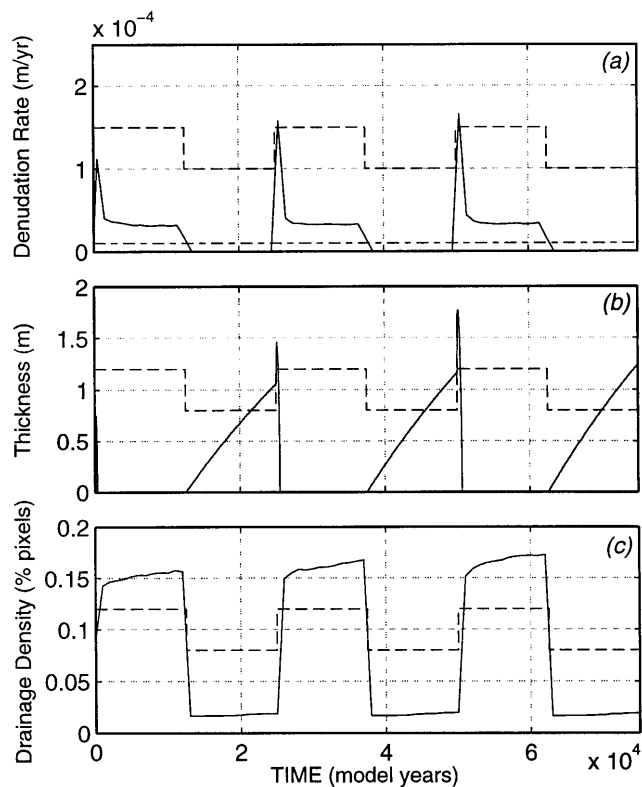

Figure 17. Basin response to short-period step-function variations in runoff intensity (see Table 2). (a) Mean basin denudation rate. (b) Sediment thickness at a representative point along the main channel network. (c) Drainage density, defined as the proportion of model cells in which the erosion threshold is exceeded. Again, note the difference between the initial and subsequent responses. (See Figure 15 for legend).

are more subtle over short time intervals. These results therefore corroborate the hypothesis of a direction-dependent response time for hollow development [*Montgomery and Dietrich*, 1992]. The model results further suggest that this direction-dependent response time effects not only hillslope hollows, but also the entire channel network.

The model results also imply that a catchment's sensitivity to changes in drainage density depends on its prior climate history. When oscillations in network extent are rapid, sediment accumulation in unchanneled valleys during intervals of network retraction will be limited, and thus the sedimentary response to network extension will be muted. Longer oscillation times allow for greater infilling of unchanneled valleys, leading to larger sediment "pulses" during periods of network expansion. In this sense the response to a climatic (or human) perturbation may depend on the degree to which the catchment retains a "memory" of past conditions.

Conceptual models in climatic geomorphology are often couched in terms of overall humidity versus aridity. Given the presence of an erosion threshold that governs drainage density, however, the intensity of precipitation during large storms may be at least as significant as mean precipitation and temperature. In the model the cycle of rapid valley aggradation and degradation that accompanies an increase in runoff intensity can occur during either a shift toward overall humidity or a shift toward aridity. Paleoclimate indicators such as pollen record primarily changes in mean or seasonally averaged temperature and humidity; the variability of rainfall in time is

Figure 16. Basin response to longer-period sinusoidal variations in runoff intensity (see Table 2). (a) Mean basin denudation rate. (b) Sediment thickness at a representative point along the main channel network. (c) Drainage density, defined as the proportion of model cells in which the erosion threshold is exceeded. Note the punctuated nature of denudation rates. (See Figure 15 for legend).

Figure 18. Basin response to longer-period step-function variations in runoff intensity (see Table 2). (a) Mean basin denudation rate. (b) Sediment thickness at a representative point along the main channel network. (c) Drainage density, defined as the proportion of model cells in which the erosion threshold is exceeded. Note the aggradational spike immediately following each increase in runoff intensity, which is followed by rapid downcutting and a short period of accelerated denudation. (See Figure 15 for legend).

generally much more difficult to reconstruct. The importance of precipitation variability as opposed to overall humidity may thus help to explain why different geomorphic responses (e.g., channel aggradation versus degradation) have been correlated with similar paleoclimate conditions (e.g., increasing aridity) in different parts of the world.

Many conceptual models in climatic geomorphology also assume that a single change in climate (such as an increase in humidity) will produce a single, linear result (such as channel incision). One of the most intriguing features to emerge from the model simulations is the nonlinear response to changes in the balance between erosivity (storm magnitude) and erodibility (critical shear stress). Regardless of how mean precipitation changes, increases in storm magnitude and/or decreases in surface resistance lead to sequential aggradation and erosion along the main valley network. The sequence of events observed in the model resembles the conceptual model of *Bull* [1979]. To explain an early Holocene episode of valley alluviation followed by downcutting in valleys in the southwestern United States, Bull proposed that the reduction of moisture at the Pleistocene-Holocene transition led to a reduction in vegetation cover. Reduction of vegetation increased the size and quantity of sediment delivered to the fluvial system (perhaps through an increase in drainage density) and led to valley alluviation and increased stream gradients. As soil thickness

was reduced and bedrock was increasingly exposed, sediment flux dropped off while runoff increased further, leading to valley incision. Thus, in Bull's model, a single climatic shift can lead to consecutive valley alluviation and downcutting, consistent with the results of the numerical model. Sequential rapid aggradation and erosion were also observed by *Smith* [1982] in the context of Holocene Nigerian gully evolution and were correlated with an increase in precipitation. *Smith* [1982] attributed the changeover from deposition to erosion to delayed vegetation regrowth, but in light of the model results, such a changeover may be likely to occur even in the absence of revegetation.

Different parts of a catchment may respond differently to the same external change. In the "vegetation loss" simulation the point of crossover from deposition to erosion propagates downstream through time as the sediment reservoir in the channel network becomes progressively exhausted (e.g., Figure 13). Deposition and erosion are therefore active simultaneously in different parts of the fluvial system. Such time-transgressive behavior has obvious implications for interpretation and time correlation of alluvial cut-and-fill sequences.

Given the model's sensitivity to changes in average storm magnitude, it is worth considering how much storm magnitude typically varies over intermediate to long timescales. A study by *Knox* [1984] of streams in the upper Mississippi River valley suggests that small changes in average climate variables such as mean annual temperature and precipitation are often accompanied by much larger changes in the magnitude and frequency of large floods. For example, on the Mississippi River near St. Paul, Minnesota, the magnitude of the 5% probability flood, measured on a decadal scale, varied from less than 1500 m^3 s^{-1} to over 2200 m^3 s^{-1} during the period 1860–1980, while the magnitude of the mean flood changed relatively little during the same period [*Knox*, 1984]. Thus it is reasonable to expect that even larger Holocene-scale climatic variations should have a significant impact on patterns of erosion and sedimentation within drainage basins. This seems to be borne out by studies of Holocene alluvial stratigraphy and paleoclimate [e.g., *Knox*, 1972, 1984; *Brakenridge*, 1980; *Blum and Valastro*, 1989].

The model results can be compared with studies of dated alluvial terrace sequences. *Brakenridge* [1980] used radiocarbon dating on buried floodplain paleosols to reconstruct the floodplain elevation history along the Pomme de Terre River in southern Missouri (Figure 19). The terrace dates indicate a period of stability in the early Holocene, followed by a series of erosional and depositional cycles in the late Holocene. Uncertainties in time correlation notwithstanding, the latter appear to be characterized by periods of gradual aggradation interrupted by rapid downcutting. The shape of these aggradational pulses bears a resemblance to the pulses observed in the model (Figures 16 and 18), and they may have a similar origin. *Brakenridge* [1980] attributed the late Holocene floodplain destabilization to increased storm activity, reflecting intensified meridionality of upper atmosphere circulation over the U.S. midcontinent. This hypothesis is consistent with the model results in that increases in runoff intensity are predicted to be associated with rapid deposition and (especially) erosion. It is notable that the erosional episodes charted by *Brakenridge* [1980] are correlated in time with Alpine "little ice ages." The model results would support the interpretation that the terrace tops correspond to the onset of periods of increased runoff intensity that probably accompanied these climatic events.

The model results are also consistent with the Pleistocene
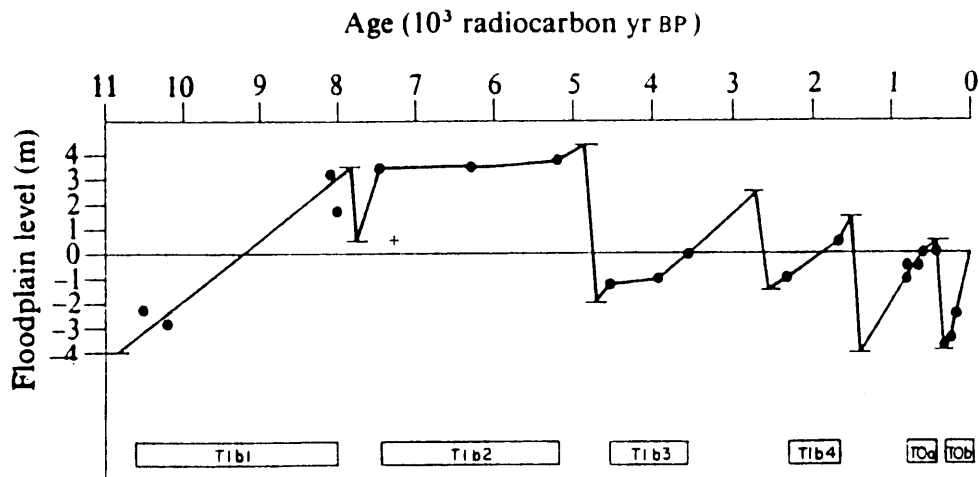
Figure 19. Plot of the floodplain elevation history of the Pomme de Terre River in southern Missouri, estimated from radiocarbon terrace dates by *Brakenridge* [1980]. Solid circles are radiocarbon ages. The plus denotes a single date that is unreliable due to a large laboratory standard deviation. The horizontal bars are estimated ages of terrace tops and bases. Note the similarity between the later Holocene aggradational-degradational episodes and the aggradational-degradational cycles produced by the model (Figures 15–18). (Reproduced from *Brakenridge* [1980]. Copyright 1980 by Macmillan Magazines Limited; reprinted with permission.)

river terrace data of *Sugai* [1993] from the Usui River, in central Japan. Pleistocene cut-and-fill terraces along the Usui River appear to be associated with glacial cycles, with alluviation occurring during glacial periods and bedrock straths forming during interglacials. On the basis of paleohydrologic analysis of terrace gravels, *Sugai* [1993] demonstrated that these cut-and-fill cycles are correlated with changes in bed shear stress associated with the presence or absence of typhoons. *Sugai* [1993] also noted that the fill terrace profiles along the Usui River are markedly less concave than either the strath profiles or the modern river profile, which is again consistent with the model's predicted variations in concavity between bedrock and alluvial longitudinal profiles.

On a shorter timescale, *Orbock Miller et al.* [1993] observed that historical aggradation (1860s to 1920s) accompanied deforestation and upland erosion within the Drury Creek watershed, in southern Illinois. Aggradation was followed by an episode of channel incision that coincided with both watershed revegetation and with a period of increased storm activity. The aggradational phase appears to reflect an increase in sediment supply to the channel network, and thus it corresponds to the aggradational phase seen in the reduced vegetation simulation (Figure 13). The observed changeover from aggradation to erosion following the reduction in sediment supply from headwaters and an increase in storm activity is also consistent with the model's behavior.

Some of the observed changes in Holocene fluvial systems are inferred to be the result of rather subtle changes in mean climate. For example, the Holocene changes in bankfull discharge and fluvial behavior in western Wisconsin streams discussed by *Knox* [1972; 1984] are inferred, on the basis of fossil pollen, to have occurred during a gradual relative warming of 1°–2°C. This magnitude of change is well within the range of changes predicted by global climate models in response to a doubling of atmospheric CO_2 [e.g., *Mitchell et al.*, 1990; *Giorgi et al.*, 1994]. The nested climate model of *Giorgi et al.* [1994], for example, predicts average winter temperature increases of between 3° and 8°C over North America in response to a CO_2

doubling. Predicted regional effects include increased summer storm activity over northern Mexico, Texas, the eastern plains, and the Great Lakes area. The Holocene record suggests that these types of continental- and regional-scale climatic changes are capable of having a significant impact on fluvial systems.

In total, the model experiments presented herein suggest that changes in drainage density due to interactions between hillslopes and first-order channels exert a fundamental control on the larger branches of the fluvial system. One means of testing the various scenarios suggested by the numerical simulations would be to combine investigations of alluvial stratigraphy on larger streams with studies of contemporaneous changes in hillslope colluviation and channel network extent, such as that by *Reneau et al.* [1986].

Conclusions

The theory embodied in this model predicts several important characteristics of a catchment's geomorphic response to climate change. Where channel network extent is controlled by a threshold for flow-driven erosion, a catchment will respond much more rapidly to an increase in the intensity of runoff (or to a decrease in critical shear stress brought about, for example, by vegetation loss) than to the reverse. This directional sensitivity implies a potential for punctuated catchment evolution in response to smoothly varying climate.

To the degree that the model's sensitivity to runoff intensity is real, the results underscore the importance of the distribution of precipitation in time, as opposed to mean precipitation. Independent evidence indicates that relatively small changes in mean climate are often accompanied by large fluctuations in the frequency and magnitude distribution of larger storms. The present model may, however, overstate the sensitivity to runoff intensity via the assumption of a single-size repeated storm event. The role of variable storm size and recurrence interval in the context of this model remains as an important issue for further study.

The model results also imply that basin responses, particu-

larly in terms of valley erosion and deposition, may be nonlinear. Through feedbacks between hillslope and channel processes, a single perturbation may lead to sequential aggradation and erosion along a valley network. This finding accords with field evidence for rapid fluvial deposition followed by downcutting in response to Quaternary climate change, and it casts doubt on the usefulness of simple conceptual models that postulate a one-to-one correspondence between a given climate state (such as increased humidity) and a given geomorphic response (such as valley aggradation).

The results from this model also have implications for basin sediment-yield studies. For a threshold-dominated drainage basin the model predicts that significant variations in sediment flux and (equivalently) in denudation rate can accompany relatively modest variations in runoff or surface resistance. The maximum denudation rate during a climate cycle is predicted to coincide in time with increasing runoff intensity (or decreasing vegetation cover). Sediment flux and denudation rate are likely to show much more variability than basin relief and morphology in response to climate variation, reflecting the difference in timescales associated with changes in drainage density and regolith thickness as opposed to changes in overall basin relief. Because first-order channels provide the conduits for sediment delivery to the river network, changes in drainage density can produce large transient variations in sediment yield. This finding underscores the difficulty in estimating long-term denudation rates from short-term sediment yield measurements, particularly from threshold-dominated basins of the type considered here.

References

Ahnert, F., Brief description of a comprehensive three-dimensional process-response model of landform development, *Z. Geomorphol.*, Suppl., *25*, 29–49, 1976.

Alley, R. B., et al., Abrupt increase in Greenland snow accumulation at the end of the Younger Dryas event, *Nature*, *362*, 527–529, 1993.

Anderson, R. S., and N. F. Humphrey, Interaction of weathering and transport processes in the evolution of arid landscapes, in *Quantitative Dynamic Stratigraphy*, edited by T. Cross, pp. 349–361, Prentice-Hall, Englewood Cliffs, N. J., 1990.

Antevs, E., Arroyo-cutting and filling, *J. Geol.*, *60*, 375–385, 1952.

Arbogast, A. F., and W. C. Johnson, Climatic implications of the late Quaternary alluvial record of a small drainage basin in the central Great Plains, *Quat. Res.*, *41*, 298–305, 1994.

Armstrong, A. C., A three-dimensional simulation of slope forms, *Z. Geomorphol.*, Suppl., *25*, 20–28, 1976.

Bloom, A. L., *Geomorphology: A systematic analysis of late Cenozoic landforms*, 2nd ed., 532 pp., Prentice Hall, Englewood Cliffs, N. J., 1991.

Blum, M. D., and S. Valastro Jr., Response of the Pedernales River of central Texas to late Holocene climatic change, *Ann. Assoc. Am. Geogr.*, *79*, 435–456, 1989.

Brakenridge, G. R., Widespread episodes of stream erosion during the Holocene and their climatic cause, *Nature*, *283*, 655–656, 1980.

Bridge, J. S., and D. D. Dominic, Bed load grain velocities and sediment transport rates, *Water Resour. Res.*, *20*, 476–490, 1984.

Bryan, K., Historic evidence on changes in the channel of the Rio Puerco, a tributary of the Rio Grande in New Mexico, *J. Geol.*, *36*, 265–282, 1928.

Bryan, K., Erosion in the valleys of the Southwest, *N. M. Q.*, *10*, 227–232, 1940.

Bull, W. B., Threshold of critical power in streams, I, *Geol. Soc. Am. Bull.*, *90*, 453–464, 1979.

Bull, W. B., *Geomorphic Responses to Climatic Change*, 326 pp., Oxford Univ. Press, New York, 1991.

Colman, S. M., and K. Watson, Ages estimated from a diffusion equation model for scarp degradation, *Science*, *221*, 263–265, 1983.

Dietrich, W. E., C. J. Wilson, D. R. Montgomery, J. McKean, and R. Bauer, Erosion thresholds and land surface morphology, *Geology*, *20*, 675–679, 1992.

Dietrich, W. E., C. J. Wilson, D. R. Montgomery, and J. McKean, Analysis of erosion thresholds, channel networks, and landscape morphology using a digital terrain model, *J. Geol.*, *101*, 259–278, 1993.

Dietrich, W. E., R. Reiss, M.-L. Hsu, and D. R. Montgomery, A process-based model for colluvial soil depth and shallow landsliding using digital elevation data, *Hydrol. Processes*, *9*, 383–400, 1995.

Dohrenwend, J. C., Basin and range, in *Geomorphic Systems of North America*, *Geol. Soc. of Am. Centen. Spec. Vol. 2*, edited by W. L. Graf, pp. 303–342, Geol. Soc. Am., Boulder, Colo., 1987.

Dorn, R. I., The role of climatic change in alluvial fan development, in *Geomorphology of Desert Environments*, edited by A. D. Abrahams and A. J. Parsons, pp. 593–615, Chapman and Hall, New York, 1994.

Dorn, R. I., M. J. DeNiro, and H. O. Ajie, Isotopic evidence for climatic influence on alluvial-fan development in Death Valley, California, *Geology*, *15*, 108–110, 1987.

Douglas, I., Man, vegetation, and the sediment yield of rivers, *Nature*, *215*, 925–928, 1967.

Fairbridge, R. W., *Encyclopedia of Geomorphology*, Reinhold, New York, 1968.

Flint, J. J., Stream gradient as a function of order, magnitude, and discharge, *Water Resour. Res.*, *10*, 969–973, 1974.

Freeze, R. A., Modelling interrelationships between climate, hydrology, and hydrogeology and the development of slopes, in *Slope Stability*, edited by M. G. Anderson, and K. S. Richards, pp. 381–403, John Wiley, New York, 1987.

Gilbert, G. K., Report on the geology of the Henry Mountains, U.S. Geogr. and Geol. Surv. of the Rocky Mt. Reg., Washington, D. C., 1877.

Giorgi, F., C. S. Brodeur, and G. T. Bates, Regional climate change scenarios over the United States produced with a nested regional climate model, *J. Clim.*, *7*, 375–400, 1994.

Goudie, A., *The Human Impact on the Natural Environment*, 3rd ed., Blackwell, Cambridge, Mass., 1990.

Graf, W. H., *Hydraulics of Sediment Transport*, 513 pp., McGraw-Hill, New York, 1971.

Hall, S. A., Channel trenching and climatic change in the southern U.S. Great Plains, *Geology*, *18*, 342–345, 1990.

Hanks, T. C., R. C. Bucknam, K. R. Lajoie, and R. E. Wallace, Modification of wave-cut and faulting-controlled landforms, *J. Geophys. Res.*, *89*, 5771–5790, 1984.

Horton, R. E., Erosional development of streams and their drainage basins: Hydrophysical approach to quantitative morphology, *Geol. Soc. Am. Bull.*, *56*, 275–370, 1945.

Howard, A. D., A detachment-limited model of drainage basin evolution, *Water Resour. Res.*, *30*, 2261–2285, 1994.

Howard, A. D., Thresholds and bistable states in landform evolution models, *Eos Trans. AGU*, *77*(17), Spring Meet. Suppl., 136, 1996.

Howard, A. D., and G. Kerby, Channel changes in badlands, *Geol. Soc. Am. Bull.*, *94*, 739–752, 1983.

Huntington, E., The climatic factor as illustrated in arid America, *Publ. 192*, Carnegie Inst., Washington, D. C., 1914.

Kirkby, M. J., Thresholds and instability in stream head hollows: A model of magnitude and frequency for wash processes, in *Process Models and Theoretical Geomorphology*, edited by M. J. Kirby, pp. 295–314, John Wiley, New York, 1994.

Knox, J. C., Valley alluviation in southwestern Wisconsin, *Ann. Assoc. Am. Geogr.*, *62*, 401–410, 1972.

Knox, J. C., Responses of river systems to Holocene climates, in *Late Quaternary Environments of the United States*, vol. 2, *The Holocene*,

edited by H. E. Wright and S. C. Porter, pp. 26–41, Univ. of Minn. Press, Minneapolis, 1983.

Knox, J. C., Fluvial responses to small-scale climatic changes, in *Developments and Applications of Geomorphology*, edited by J. E. Costa and P. J. Fleisher, pp. 318–342, Springer-Verlag, New York, 1984.

Langbein, W. B., and S. A. Schumm, Yield of sediment in relation to mean annual precipitation, *Eos Trans. AGU*, *39*, 1076–1084, 1958.

Leopold, L. B., Rainfall frequency: An aspect of climatic variation, *Eos Trans. AGU*, *32*, 347–357, 1951.

Leopold, L. B., Reversal of the erosion cycle and climatic change, *Quat. Res.*, *6*, 557–562, 1976.

McKean, J. A., W. E. Dietrich, R. C. Finkel, J. R. Southon, and M. W. Caffee, Quantification of soil production and downslope creep rates from cosmogenic ^{10}Be accumulations on a hillslope profile, *Geology*, *21*, 343–346, 1993.

Meyer, G. A., S. G. Wells, R. C. Balling Jr., and A. J. T. Jull, Response of alluvial systems to fire and climate change in Yellowstone National Park, *Nature*, *357*, 147–150, 1992.

Mitchell, J. F. B., S. Manabe, V. Meleshko, and T. Tokioka, Equilibrium climate change and its implications for the future, in *Climate Change: The IPCC Scientific Assessment*, edited by J. T. Houghton, G. J. Jenkins, and J. J. Ephraums, Cambridge Univ. Press, New York, 1990.

Monaghan, M. C., J. McKean, W. Dietrich, and J. Klein, ^{10}Be chronometry of bedrock-to-soil conversion rates, *Earth Planet. Sci. Lett.*, *111*, 483–492, 1992.

Montgomery, D. R., and W. E. Dietrich, Source areas, drainage density, and channel initiation, *Water Resour. Res.*, *25*, 1907–1918, 1989.

Montgomery, D. R., and W. E. Dietrich, Channel initiation and the problem of landscape scale, *Science*, *255*, 826–830, 1992.

Montgomery, D. R., and W. E. Dietrich, Landscape dissection and drainage area-slope thresholds, in *Process Models and Theoretical Geomorphology*, edited by M. J. Kirby, pp. 221–246, John Wiley, New York, 1994.

Montgomery, D. R., T. B. Abbe, J. M. Buffington, N. P. Peterson, K. M. Schmidt, and J. D. Stock, Distribution of bedrock and alluvial channels in forested mountain drainage basins, *Nature*, *381*, 587–589, 1996.

Nash, D. B., Morphologic dating of degraded normal fault scarps, *J. Geol.*, *88*, 353–360, 1980.

Ollier, C. D., *Weathering*, 2nd ed., 270 pp., Longman, White Plains, N. Y., 1984.

Orbock Miller, S., D. F. Ritter, R. C. Kochel, and J. R. Miller, Fluvial responses to land-use changes and climatic variations within the Drury Creek watershed, southern Illinois, *Geomorphology*, *6*, 309–329, 1993.

Pazzaglia, F. J., and T. W. Gardner, Late Cenozoic flexural deformation of the middle U.S. Atlantic passive margin, *J. Geophys. Res.*, *99*, 12,143–12,157, 1994.

Reneau, S. L., W. E. Dietrich, R. I. Dorn, C. R. Berger, and M. Rubin, Geomorphic and paleoclimatic implications of latest Pleistocene radiocarbon dates from colluvium-mantled hollows, California, *Geology*, *14*, 655–658, 1986.

Rinaldo, A., W. E. Dietrich, R. Rigon, G. Vogel, and I. Rodriguez-Iturbe, Geomorphological signatures of varying climate, *Nature*, *374*, 632–634, 1995.

Rosenbloom, N. A., and R. S. Anderson, Hillslope and channel evo-

lution in a marine terraced landscape, Santa Cruz, California, *J. Geophys. Res.*, *99*, 14,013–14,030, 1994.

Schumm, S. A., *The Fluvial System*, 338 pp., John Wiley, New York, 1977.

Slingerland, R. L., and R. S. Snow, Stability analysis of a rejuvented fluvial system, *Z. Geomorphol.*, Suppl., *67*, 93–102, 1988.

Slingerland, R. L., J. W. Harbaugh, and K. P. Furlong, *Simulating Clastic Sedimentary Basins*, 220 pp., Prentice-Hall, Englewood Cliffs, N. J., 1993.

Smith, B. J., Effects of climate and land-use change on gully development: An example from northern Nigeria, *Z. Geomorphol.*, Suppl., *44*, 33–51, 1982.

Strahler, A. N., and A. H. Strahler, *Modern Physical Geography*, 502 pp., John Wiley, New York, 1978.

Sugai, T., River terrace development by concurrent fluvial processes and climatic changes, *Geomorphology*, *6*, 243–252, 1993.

Tarboton, D. G., R. L. Bras, and I. Rodriguez-Iturbe, Scaling and elevation in river networks, *Water Resour. Res.*, *25*, 2037–2051, 1989.

Taylor, K. C., et al., The "flickering switch" of late Pleistocene climate change, *Nature*, *361*, 432–436, 1993.

Tucker, G. E., Modeling the large-scale interaction of climate, tectonics, and topography, *Tech. Rep. 96-003*, Penn. State Univ. Earth Syst. Sci. Cent., University Park, 1996.

Tucker, G. E., and R. L. Slingerland, Erosional dynamics, flexural isostasy, and long-lived escarpments: A numerical modeling study, *J. Geophys. Res.*, *99*, 12,229–12,243, 1994.

Tucker, G. E., and R. L. Slingerland, Predicting sediment flux from fold and thrust belts, *Basin Res.*, *8*, 329–349, 1996.

Vita-Finzi, C., *The Mediterranean Valleys*, 140 pp., Cambridge Univ. Press, New York, 1969.

Willgoose, G. R., A physically based channel network and catchment evolution model, Ph.D. thesis, 464 pp., Mass. Inst. of Technol., Cambridge, 1989.

Willgoose, G. R., A statistic for testing the elevation characteristics of landscape simulation models, *J. Geophys. Res.*, *99*, 13,987–13,996, 1994.

Willgoose, G. R., R. L. Bras, and I. Rodriguez-Iturbe, Results from a new model of river basin evolution, *Earth Surf. Processes Landforms*, *16*, 237–254, 1991.

Wilson, L., Variations in mean annual sediment yield as a function of mean annual precipitation, *Am. J. Sci.*, *273*, 335–349, 1973.

Yalin, M. S., *Mechanics of Sediment Transport*, 2nd ed., 298 pp., Pergamon, Tarrytown, N. Y., 1977.

Yalin, M. S., *River Mechanics*, 219 pp., Pergamon, Tarrytown, N. Y., 1992.

Yang, C. T., *Sediment Transport: Theory and Practice*, 396 pp., McGraw-Hill, New York, 1996.

R. Slingerland, Department of Geosciences and Earth System Science Center, Pennsylvania State University, University Park, PA 16802.

G. E. Tucker, Ralph M. Parsons Laboratory, Massachusetts Institute of Technology, Room 48-108, Cambridge, MA 02139. (e-mail: gtucker@mit.edu)